City Research Online

City, University of London Institutional Repository

Citation: Silipo, D., Greggio, J. & Malamateniou, C. (2026). The role of AI in optimizing CMR image quality: A scoping review. Journal of Medical Imaging and Radiation Sciences, 57(1), 102135. doi: 10.1016/j.jmir.2025.102135

This is the published version of the paper.

This version of the publication may differ from the final published version.

Permanent repository link: https://openaccess.city.ac.uk/id/eprint/36410/

Link to published version: https://doi.org/10.1016/j.jmir.2025.102135

Copyright: City Research Online aims to make research outputs of City, University of London available to a wider audience. Copyright and Moral Rights remain with the author(s) and/or copyright holders. URLs from City Research Online may be freely distributed and linked to.

Reuse: Copies of full items can be used for personal research or study, educational, or not-for-profit purposes without prior permission or charge. Provided that the authors, title and full bibliographic details are credited, a hyperlink and/or URL is given for the original metadata page and the content is not changed in any way.

City Research Online: http://openaccess.city.ac.uk/ publications@city.ac.uk

Journal of Medical Imaging and Radiation Sciences 57 (2026) 102135

Journal of Medical Imaging and Radiation Sciences

Journal de l'imagerie médicale et des sciences de la radiation

www.elsevier.com/locate/jmir

Scoping Review

The role of AI in optimizing CMR image quality: A scoping review

Daniele Silipo [a,*], Julien Greggio [b,c] and Christina Malamateniou [c]

[a] *Alliance Medical- City St George's, University of London, Northampton Square, London EC1V 0HB, United Kingdom*
[b] *City St George's, University of London – Everything MRI London, UK*
[c] *City St George's, University of London, UK*

ABSTRACT

Background: Cardiovascular magnetic resonance (CMR) imaging is a powerful tool for assessing cardiac anatomy and function but remains limited by average image quality due to artefacts and long acquisition times, and complex and often too long breath-holds. Deep learning methods have recently been applied and show potential to shorten scan times by 70–80 % while improving image quality, enhancing clinical efficiency. The aim of this study is to summarise the different AI-enabled methods for improving CMR image quality, including scanning time, as a key determinant for artefact reduction.

Methods: A scoping review was conducted according to PRISMA guidelines. The articles were screened and reviewed by two researchers. A qualitative thematic synthesis was conducted and a CASP-mediated risk of bias assessment was performed.

Results: The eligible articles were thirty-one. These articles were thematically categorised in four subgroups, based on emerging themes: scan acceleration, artefact detection, artefact reduction, image reconstruction. A table with significant results for each theme has been presented and results were discussed qualitatively.

Discussion: AI demonstrated consistent improvements across the four subgroups. For scan acceleration, deep learning achieved approximately a 70–80 % reduction in scan duration maintaining or even improving image quality. For artefact detection, convolutional neural networks achieved on average a 90 % accuracy in detecting artefacts, across multiple metrics, indicating reliable artefact identification and strong agreement with human experts. AI models effectively reduce artefacts and enhance image quality, achieving consistently better reconstruction accuracy, sharper edges, and faster processing compared to conventional methods. Finally, for image reconstruction, generative adversarial networks enhanced structural similarity by approximately 56 % (SSIM 0.591 → 0.925). Together, these results illustrate the potential of AI to optimise CMR image quality.

Conclusion: AI can be an effective tool in addressing many of the CMR imaging challenges and thus improving image quality.

RÉSUMÉ

Contexte: L'imagerie par résonance magnétique cardiovasculaire (IRM-CV) est un outil puissant pour évaluer l'anatomie et la fonction cardiaques, mais elle reste limitée par une qualité d'image moyenne due à des artefacts et à des temps d'acquisition longs, ainsi qu'à des apnées complexes et souvent trop longues. Des méthodes d'apprentissage profond ont récemment été appliquées et montrent un potentiel de réduction des temps de balayage de 70 à 80 % tout en améliorant la qualité de l'image, ce qui renforce l'efficacité clinique. L'objectif de cette étude est de résumer les différentes méthodes basées sur l'IA permettant d'améliorer la qualité des images IRM-CV, y compris le temps de balayage, en tant que facteur déterminant pour la réduction des artefacts.

Méthodologie: Une revue exploratoire a été réalisée conformément aux directives PRISMA. Les articles ont été sélectionnés et examinés

Abbreviations: CMR, Cardiac magnetic resonance; AI, Artificial intelligence; DL, Deep learning; ML, Machine learning; IQ, Image quality; MRI, Magnetic resonance imaging; 3D, Three-dimensional; 2D, Two-dimensional; CNN, Convolutional neural network; GAN, Generative adversarial network; VN, Variational network; Hyb-Rf, Hybrid random forest; bSSFP, balanced Steady-State Free Precession; GRE, Gradient echo; GRASP, Golden-angle RAdial Sparse Parallel imaging; CMRA, Coronary Magnetic Resonance Angiography; FLASH, Fast Low Angle Shot; MRF, Magnetic Resonance Fingerprinting; MTC-BOOST, Magnetization Transfer Contrast - Bright and black blOOd phase-SensiTive imaging; LV, Left Ventricle; RV, Right Ventricle; n, Subjects number.

Contributors: All authors contributed to the conception or design of the work, the acquisition, analysis, or interpretation of the data. All authors were involved in drafting and commenting on the paper and have approved the final version.

Funding: This study did not receive any specific grant from funding agencies in the public, commercial, or not-for-profit sectors.

Competing interests: All authors have completed the ICMJE uniform disclosure form and declare no conflict of interest.

Ethical approval: Not required for this article type.

* Corresponding author.
E-mail address: daniele.silipo.91@gmail.com (D. Silipo).

1939-8654/$ - see front matter © 2025 Published by Elsevier Inc. on behalf of Canadian Association of Medical Radiation Technologists. This is an open access article under the CC BY license (http://creativecommons.org/licenses/by/4.0/)
https://doi.org/10.1016/j.jmir.2025.102135

par deux chercheurs. Une synthèse thématique qualitative a été réalisée et une évaluation du risque de biais à l'aide du programme CASP a été effectuée.

Résultats: Au total, 31 articles admissibles ont été recensés. Ces articles ont été classés par thème en quatre sous-groupes, en fonction des thèmes émergents : accélération du balayage, détection des artefacts, réduction des artefacts, reconstruction d'images. Un tableau présentant les résultats significatifs pour chaque thème a été présenté et les résultats ont fait l'objet d'une discussion qualitative.

Discussion: L'IA a démontré des améliorations constantes dans les quatre sous-groupes. En ce qui concerne l'accélération du balayage, l'apprentissage profond a permis de réduire la durée du balayage d'environ 70 à 80 % tout en maintenant, voire en améliorant, la qualité de l'image. En ce qui concerne la détection des artefacts, les réseaux neuronaux convolutifs ont atteint en moyenne une précision de 90 % dans la détection des artefacts, selon plusieurs mesures, ce qui indique une identification fiable des artefacts et une forte concordance avec les experts humains. Les modèles d'IA réduisent efficacement les artefacts et améliorent la qualité de l'image, permettant d'obtenir une précision de reconstruction systématiquement meilleure, des contours plus nets et un traitement plus rapide par rapport aux méthodes conventionnelles. Enfin, pour la reconstruction d'images, les réseaux génératifs antagonistes ont amélioré la similarité structurelle d'environ 56 % (SSIM 0591 → 0925). Ensemble, ces résultats illustrent le potentiel de l'IA pour optimiser la qualité des images IRM-CV.

Conclusion: L'IA peut être un outil efficace pour relever bon nombre des défis liés à l'imagerie IRM-CV et ainsi améliorer la qualité des images.

Keywords: Artificial intelligence; Magnetic resonance imaging; Cardiovascular magnetic resonance imaging; Image quality optimisation; Scoping Review

Introduction

Cardiovascular magnetic resonance (CMR) imaging is an effective and non-invasive method of assessing heart anatomy and function. It is the gold standard of ventricular function and allows accurate measurements of cardiac variables such as ventricular volumes, ejection fraction, strain, and myocardial wall defects [1]. Such properties make CMR an excellent tool for diagnosing and monitoring cardiovascular conditions [2].

Despite its strengths, CMR has limitations. Image quality may be affected by patient-related factors such as arrhythmias, difficulty managing breath-holds, or movement during scans [3]. Common artefacts arise from respiratory motion, blood flow, and magnetic field inhomogeneity, requiring additional quality checks and prolonging examination times [4–6]. The quality of CMR images is strongly connected to the operator's ability to adjust parameters based on each patient's specific needs; for this reason, the operator's expertise is a crucial element for cardiovascular imaging [7].

Newer technologies, namely artificial intelligence (AI), promise to help tackle many CMR imaging challenges. AI approaches are now integrated to improve CMR imaging processes in every step, from acquisition to post-processing [2,8].

Deep learning models like convolutional neural networks (CNNs), U-Nets, and generative adversarial networks (GANs) have effectively reduced artefacts and improved image reconstruction [4]. These technologies enable shorter exams, free-breathing scans, and improved patient comfort [9]. Additionally, AI automates cardiac segmentation and functional biomarker analysis, achieving expert-level accuracy while streamlining workflows [1,10,11].

Conventional CMR acquisition techniques, such as 3D whole-heart imaging with navigator gating, often achieve only ~30–45 % scan efficiency, leading to prolonged and unpredictable acquisition times. These extended scans increase the risk of motion and other artefacts, which may compromise diagnostic accuracy. In contrast, deep learning–based reconstruction methods have demonstrated the ability to reduce scan time by approximately 70–80 % while improving image quality, thereby enhancing both efficiency and reliability in clinical CMR practice [8,10].

Aim and objectives

This scoping review aims to evaluate the existing applications of AI in CMR and how AI algorithms could be implemented into CMR pipelines to improve image quality.

Objectives:

- Identify key challenges in CMR related to image quality optimisation.
- Review and summarise studies integrating AI to CMR.
- Describe limitations in existing studies.
- Present opportunities for future research ideas in this field.

Methods

Ethical considerations

This article is a scoping review based solely on previously published literature. According to JMIRS guidelines, research based on the analysis of published data does not require ethical approval. Therefore, ethics approval was not required for this study.

Protocol

This paper adheres to a scoping review methodology and conforms to the Preferred Reporting Items for scoping review and Meta-Analyses (PRISMA) statement [12,13]. This scoping review research question was based on the PICO

framework [14]. The search for this paper was conducted between May 2024 and August 2024, and the protocol is registered with PROSPERO [15] under the ID CRD42025626450.

Sources of information

The following databases were searched: PubMed, Google Scholar, arXiv, The Cochrane Library.

Eligibility criteria

The inclusion criteria were applied to focus the review on studies published between 2019 and 2024, written in English, directly related to CMR image quality and AI, performed on human subjects, and available as full-text articles. Conversely, exclusion criteria eliminated studies not related to CMR, not employing AI, lacking a focus on image quality, not based on human data, or written in any other language different from English.

Search strategy

A comprehensive literature search was performed using relevant keywords, including "CMR," "cardiac magnetic resonance," "cardiac MRI," "machine learning," "deep learning," "AI," "artificial intelligence," "image quality," "motion correction," "motion," "artefact," and "artifact." Boolean operators such as "AND" and "OR" were used to refine the search strategy.

A medical librarian assisted with collecting and organising search materials, while the search strategy was developed collaboratively by the authors in accordance with PRISMA guidelines to ensure methodological rigor.

Qualitative synthesis

The data were analysed using qualitative thematic synthesis. In this process, the findings of each study were coded line by line and initially organised into descriptive themes, and subsequently into analytical themes [16]. Meanings and themes were then grouped and classified into four specific subcategories: scan acceleration, artefact detection, artefact reduction, and image reconstruction. For each theme, the most relevant results have been extracted from the studies and organised in a specific table. Figures that exemplify the aspect that has been analysed have been presented after the tables for a better understanding.

Risk of bias assessment & quality assurance

Given that this review employed a qualitative thematic synthesis approach, the Critical Appraisal Skills Programme (CASP) tool was utilized as a systematic and standardized framework to assess the risk of bias in the selected studies. The included articles were critically appraised to ensure their findings' validity, reliability, and relevance. Each study's research design, methods, and results have been evaluated individually to assess reliability and relevance [17]. The studies have been classified according to their risk of bias in the following groups:

- Low risk: High-quality study with properly structured research design, precise methods, and reliable results.
- Medium risk: Medium-quality study that presents some risk of bias, but it is acceptable for inclusion.
- High risk: The study is poorly designed and has an unclear protocol. There is a significant risk of bias that can affect inclusion.

To ensure inter-reviewer reliability, a second reviewer independently replicated the entire review process using the same search strategy, Boolean operators, databases, and eligibility criteria to minimise bias and confirm consistency.

Results

Study selection

From the initial 1198 articles, 401 articles were selected for the first screening after duplicates were removed. After the first screening, 284 articles were excluded, and 117 were assessed for eligibility. Of the 117 articles, 86 were excluded following the inclusion and exclusion criteria. At the full-text review stage, the main reasons for exclusion were studies focusing primarily on mathematical reconstruction algorithms rather than AI-based approaches, lack of emphasis on image quality as an outcome, use of imaging modalities other than MRI, methodological shortcomings, and population mismatch. The final number of eligible articles was 31 (Fig. 1). These articles provided the basis for the scoping review and were considered critical in understanding the role of AI in CMR image quality. This thorough approach ensured the inclusion of relevant and high-quality research focusing on recent AI developments in scan acceleration, artefact detection, artefact reduction, and image reconstruction in CMR imaging.

The research independently performed by the second reviewer yielded a total of 702 articles, of which 676 were excluded due to duplication or failure to meet the inclusion criteria. The remaining 26 studies overlapped significantly with those identified in the primary review, supporting the reliability and reproducibility of the methods used.

Study characteristics

The eligible studies have been conducted in different countries. Specifically, 11 were conducted in the United Kingdom (UK), 8 in the United States of America (USA), 5 in China, 3 in Germany, 1 in South Korea, 1 in Austria, 1 in Japan and 1 in Switzerland. All the studies have been published between 2019 and 2024. The main research design used was a technical development and validation study. The majority of the studies (12 out of 31) used a Siemens 1.5T MRI scanner, followed by GE (8 studies) and Philips (5 studies); the remaining 6 studies did not specify the scanner manufacturer. Various MR sequences were employed in the development of AI

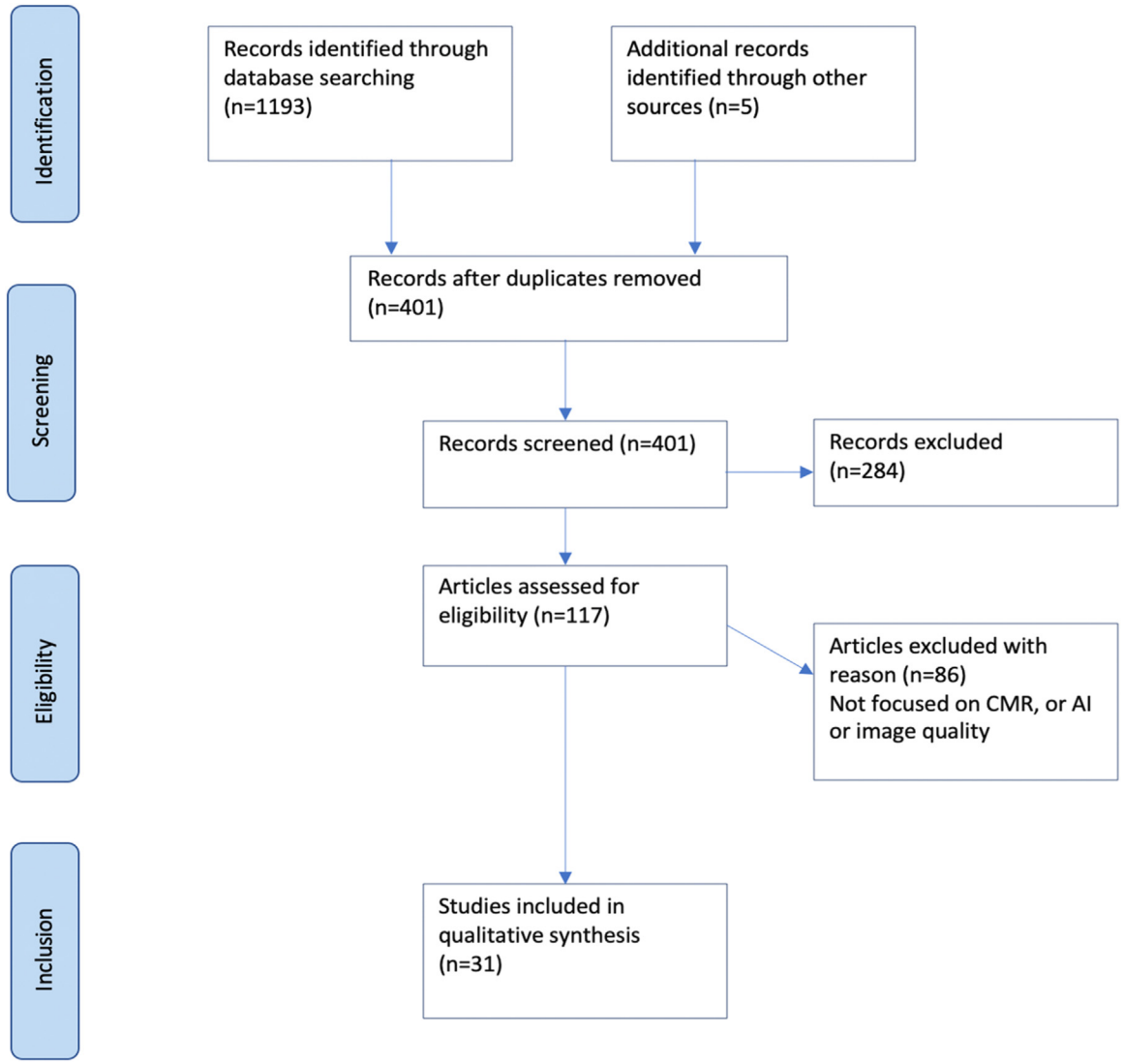

Fig. 1. PRISMA flow diagram.

algorithms, with the most commonly used being bSSFP (both 2D and 3D, used in 15 studies). Other sequences included FLASH (8 studies), T1 mapping (shMOLLI) and T2 mapping (2 studies), CMRA (7 studies), FIESTA (1 study), MRF (1 study), SSFP (4 studies), GRE (5 studies), and MTC-BOOST (1 study). Some studies tested AI algorithms with multiple MR sequences.

Studies categories

The 31 articles have been divided into 4 categories according to their topics, for a more structured results analysis.

Scan Acceleration, including breath-hold shortening: AI models aiming at reducing scan times and breath-holds as a way of reducing/preventing motion artefacts and improving overall image quality.

Artefact Detection: AI algorithms programmed to identify and evaluate motion and other artefacts in images.

Artefact Reduction: AI techniques that can improve image quality by decreasing the presence of artefacts on the images.

Image Reconstruction: AI methods that improve the quality of reconstructed images from raw data.

A table has been created for each category, detailing the AI model, algorithm name, architecture, MRI sequence, subjects' number, image quality score, feasibility and a category-specific score.

Scan acceleration, including breath-hold shortening

The following table presents the results reported from the articles selected that focus mainly on the acceleration and breath-hold optimisation (Table 1).

Among the included studies in the scan acceleration section, six CNN-based algorithms were applied to FLASH, 2D and 3D bSSFP, and MRF sequences, with a total of 84 subjects. Two DLR-based models focused on 2D bSSFP and SSFP CINE sequences, including 33 subjects. Two variational

Table 1
This table presents AI algorithms focused on acceleration, including breath-hold shortening techniques.

AI model	AI algorithm name and architecture	MRI sequence/ subjects (n)	Time / Acceleration	Image quality score	Clinical notes
CNN	**MoDL-SToRM** (iterative CNN + SToRM, CG)	FLASH / $n = 4$	Reconstruction ≈30s	PSNR (37.83–42.98),SSIM (0.9021–0.9721)	Works with limited training data; efficient and faster reconstruction.
	MoCo-MoDL (motion-estimation + denoising, iterative)	2D bSSFP CINE / $n = 8$	Scan 2.1 ± 0.3 min; Reconstruction ≈30 s; 240× faster	SSIM 0.906; median confidence 4/4; sharpness 5/5	Strong acceleration; larger datasets needed.
	DIP-MRF (U-Net + Fully connected network)	MRF / $n = 28$	Reducing scan time from 15→5 HB; 250→150 ms	Native T1 (1047 ± 46), T2 (45.7 ± 4.0); reduced artefacts	Reliable diagnostic values; needs testing on more sequences.
	4D CINENet (spatio-temporal convolutions, multi-coil)	3D bSSFP / $n = 15$	≈10 s vs 30 s (3D CINE) / 260 s (2D CINE)	Blood – myocardium contrast ratio ≈0.28 (vs 0.17 with CS) 0.32 reference in 2D CINE; +67 % IQ over iterative	Enhances quality with shorter scan time; requires broader validation.
	2D CNN (5-stage)	bSSFP / $n = 19$	Reconstruction time ~9 (s) for proposed method, 16.8 (s) for 2D CRNN cascade, 8.8 (s) for 3D CRNN cascade, 150 (s) kt-SENSE	PSNR (32.281) for proposed method, (30.383) for 2D CRNN cascade, (33.779) for 3D CRNN cascade. SSIM (0.842) for proposed method, (0.855) for 2D CRNN cascade, (0.908) for 3D CRNN cascade	Algorithm quality of images comparable, in certain case superior to, 2D CNNs and 3D CNNs, faster reconstruction time of previous model.
	EasyScan (regression CNN)	bSSFP / $n = 30$	13 % accelerated CMR scan with EasyScan (2.57 min faster) compared to manual planning, $\boldsymbol{p < 0.001}$, 95 % CI	12.49 % higher SNR and 2 % sharper images ($p = 0.002$, $p = 0.012$) compared to manual shimming	Improves planning/shimming; efficient in clinic, decreasing scan time.
DLR	**DLR**	2D bSSFP / $n = 24$	Time of acquisition (s), bSSFP (327.6 ± 65.8) with DLR (41.0 ± 11.3), motion artefact bSSFP (4.5 ± 0.7) with DLR (3.9 ± 0.4) $\boldsymbol{p < 0.0001}$	Blood to myocardial contrast bSSFP (4.9 ± 0.3) with DLR (4.8 ± 0.4), endocardial edge definition (4.5 ± 0.7) with DLR (4.1 ± 0.5)	CINE sequence acceleration, slightly lower image quality compared to standard CINE, data only for short axis.
	Sonic DL CINE	SSFP CINE / $n = 9$	21–76 s vs 150 ± 34 s (standard CNE)	No statistically significant difference ($\boldsymbol{p > 0.198}$ **or higher**)	Fastest acquisition; preserves quality.
VN	**jMS-VNN** (10-stage iterative reconstruction)	3D MTC-BOOST / $n = 36$	Improved scan time, 3 min (±1 min), and reconstruction time, 20 s (±2 s)	PSNR (47.39 ± 2.5), SSIM (0.72 ± 0.1) $\boldsymbol{p < 0.001}$	Improved image quality compared to CS, short acquisition time.
	GC-VN (model-based variational network with conjugate gradient)	CMRA, MTC-BOOST / $n = 20$	Reconstruction 35 s (CMRA), 19 s (MTC-BOOST); 30 and 47 % faster	PSNR (31.5 ± 2.7); +29 % signal vs prior	Scan time reduction and signal improvement.

network models were tested on 3D MTC-BOOST and CMRA, with 56 subjects overall.

CNN: MoDL-SToRM enabled fast reconstruction in ≈30 s. MoCo-MoDL achieved scan acceleration of ≈240× (2.1 ± 0.3 min). DIP-MRF reduced acquisition from 15 to 5 heartbeats. The 2D CNN reconstructed images in ≈9 s, and 4D CINENet enabled CINE imaging in ≈10 s. EasyScan shortened scans by 13 % (≈2.57 min).

DLR: DLR reduced acquisition from 327.6 ± 65.8 s to 41.0 ± 11.3 s, and Sonic DL CINE shortened acquisition to 21–76 s (vs 150 ± 34 s).

VN: Variational networks achieved reconstruction in 19–35 s, with jMS-VNN acquiring scans in 3 ± 1 min and GC-VN accelerating reconstruction by 30–47 %.

Artefact detection

The table below shows the results from selected articles that primarily focus on artefacts detection (Table 2).

Among the included studies in the artefact detection section, two CNN-based models (IQ-DCNN and 3D ResNet-50) are applied to 3D b-SSFP whole heart and 2D b-SSFP

Table 2
This table showcases AI algorithms aimed at artefact detection.

AI model	AI algorithm name and architecture	MRI sequence/ subjects (n)	Artefacts detection score	Image quality score	Clinical notes
CNN	**IQ-DCNN** (4 convolutional layers, 3 fully connected layers, 1 final regression layer; based on the VGG-16 model)	3D b-SSFP whole heart / $n = 100$	Can detect images with least amount of blurring, very good agreement with human expert (100 % agreement in detecting best quality phase),	($R2 = 0.78$, $k = 0.67$)	Requires expert reference images for clinical use.
	3D ResNet-50 (PyTorch)	2D b-SSFP CINE / $n = 269$	motion artefacts detection AUROC 0.87–0.90	Strong agreement with experts (AUROC 0.88–0.93) **$p < 0.001$**	Promising for motion/planning artefacts; workflow integration needed.
Hyb-RF	**Hybrid random forest** (decision tree structure with different kind of nodes performing multiple tasks)	2D b-SSFP CINE / $n = 3100$	Inter-slice motion artefacts (sensitivity = 78 %−85 % and specificity = 90 %−95 %)	High accuracy of contrast and coverage estimation. For coverage estimation sensitivity (88 %−100 %) specificity (99 %−100 %)	Real-time assessment feasible; lacks quality checks on imaging manual selection.
DML	**Deep Meta Learning** (ResNet18 network and a classifier network with three modules, each with fully connected layer, ReLU and batch normalisation)	2D b-SSFP CINE, FIESTA / $n = 6033$	Respiratory and cardiac motion detection. Aliasing and Gibbs ringing artefacts, accuracy (56.51 %−99.28 %) precision (55.43 %−99.46 %) f-measure (55.06 %−99.36 %)	Precise detection of artefacts, results make this model superior to previous models used	Effective for quality control; larger datasets needed for other artefacts.

CINE sequences, including a total of 369 subjects. One Hybrid Random Forest (Hyb-RF) model was tested on 2D b-SSFP CINE with 3100 subjects, while one Deep Meta-Learning (DML) model was applied to 2D b-SSFP CINE and FIESTA sequences, including 6033 subjects.

CNN: IQ-DCNN detected blurred images with $R^2 = 0.78$ and $\kappa = 0.67$. 3D ResNet-50 achieved AUROC 0.87–0.90 (overall 0.88–0.93).

Hyb-RF: Hybrid RF reached 78–85 % sensitivity and 90–95 % specificity for inter-slice motion, with up to 100 % accuracy for contrast and coverage.

DML: Deep Meta Learning achieved accuracy 56–99 %, precision 55–99 %, and F-measure 55–99 %.

Artefact reduction

The table below presents the results from selected articles that focus on artefacts reduction (Table 3).

In the artefact reduction section a total of seven CNN-based algorithms were identified, tested on CINE, bSSFP, PCMR, ShMOLLI T1 maps, and FLASH sequences, with a combined study population of 4707 subjects. One HM-based algorithm was reported, applied to bSSFP sequences with 4000 subjects.

CNN: 3D CNN and LRCN achieved recall 467–533, precision 713–724, and ROC 0.89 on CINE sequences. U-Net showed MAE 0.0417 and SSIM 0.85 on PCMR. Combined CNN/CRNN/U-Net reached segmentation overlaps of LV 0.964, myocardium 0.775, RV 0.933, with SSIM 0.623 → 0.793. RT U-Net had motion/artefact scores 4.3–4.6. Residual U-Nets recorded MAE <0.05, SSIM 0.7–1. MOCOnet reduced motion scores from 37.1 ± 21 to 13.3 ± 10.5. DEBLUR achieved HFEN 0.18 ± 0.13 and SSIM 0.96 ± 0.04.

HM: HM increased sharpness by 7 % and SSIM from 0.76 to 0.93.

Image reconstruction

The table below summarizes the results from selected articles that primarily investigate image reconstruction (Table 4).

In the image reconstruction section a total of five CNN-based algorithms were reported, tested across CINE, bSSFP, CMRA, and T1/T2W sequences, with a combined subject population of 1389. A PG-DL algorithm was tested on 11 subjects. One GAN-based model (SRGAN) was applied to 3D bSSFP (CMRA) in 31 subjects, and one HM-based approach (DnSRGAN) was tested in 64 subjects. In addition, another hybrid method (MCMR) using CNN and CG-SENSE was applied to 2D bSSFP in 886 subjects.

CNN:U-Net and ResNet achieved SNR 0.983–0.994 and SSIM 0.964–0.991, with mean quality scores of 1.40 and 2.44 (1–5 scale), respectively. MoCo-MoDL for CMRA sequences showed PSNR 27.86 ± 3.00, SSIM 0.78 ± 0.06, and a mean quality score of 3.56 ± 0.53. For 2D CINE sequences, DCCNN achieved PSNR 30.9 ± 0.07 and SSIM 0.90 ± 0.04. CRNN presented NMSE 0.0277–0.0408, PSNR

Table 3
This table highlights AI algorithms designed for artefact reduction.

AI model	AI algorithm name and architecture	MRI sequence/ subjects (n)	Artefact improvement score	Image quality score	Clinical notes
CNN	**3D CNN** (8 layers) and LRCN	CINE / $n = 10$	3DCNN R (motion artefacts) 467 ± 82, LRCN R (motion artefacts) 533 ± 65; *R = recall (proportion of artefact images correctly classified), LRCN–Curriculum BA (Mis-triggering and Arrythmia) 752 ± 114, *BA = balanced accuracy. Also Recon. Time ∼ 3.9 (s) for U-Net, ∼59 (s) CS	3DCNN P (motion artefacts) 713 ± 69, LRCN P (motion artefacts) 724 ± 57; *P = precision (proportion of correctly classified good quality images) (ROC curve 0.89) **$P < 0.05$**	Detects and improves motion artefacts with efficient reconstruction.
	U-Net	PCMR / $n = 20$	Edge sharpness 0.083 ± 0.026 (U-Net MAE), 0.101 ± 0.034 (U-Net SSIM), 0.119 ± 0.037 (CS), 0.136 ± 0.033 (Cartesian)	U-Net MAE: MAE (0.0417), PSNR (25.3), Avg. SSIM (0.85). U-Net SSIM: MAE (0.0448), PSNR (24.6), Avg. SSIM (0.86)	Improvements in removing aliasing artefact and accelerating the scan.
	CNN for image motion artefact detection, CRNN for image reconstruction, U-Net for image segmentation	2D CINE / $n = 3510$	Segmentation overlap: **Baseline** 0.889 (LV), 0.561 (Myo), 0.905 (RV), **Cascaded U-Nets** 0.895 (LV), 0.651 (Myo), 0.918 (RV), **Proposed** 0.964 (LV), 0.775 (Myo), 0.933 (RV). *baseline overlap manual segmentation and ground truth	SSIM: baseline (0.623), Cascade U-Nets (0.753), Proposed (0.793)	Artefacts detection and correction with high accuracy segmentation.
	RT U-Net (residual U-Net model)	bSSFP / $n = 770$	**BH-bSSFP:** motion (4.8 ± 0.40) artefact (4.9 ± 0.30). **RT U-Net:** motion (4.3 ± 0.46) artefact (4.6 ± 0.49). 5 points Likert scale **$P < 0.007$**	**BH-bSSFP:** edge sharpness (0.66 ± 0.15) endocardial border sharpness (4.7 ± 0.45). **RT U-Net:** edge sharpness (0.55 ± 0.14) endocardial border sharpness (4.2 ± 0.75). 5 points Likert scale. Recon. time faster >5× than CS	Improve reconstruction time and reduce artefacts, maintaining quality similar to baseline.
	Residual U-Net	bSSFP / $n = 192$	MAE reconstructions <0.05, MAE gridded between 0.05 and 0.1	SSIM reconstructions between 0.7 and 1, SSIM gridded between 0.05 and 0.2 and 0.6	both specific and generic networks offer improvements in accuracy and similarity over the gridded baseline.
	MOCOnet (U-Net architecture with warping layers)	ShMOLLI T1 maps / $n = 200$	Motion scores before motion correction 37.1 ± 21. **MOCOnet** 13.3 ± 10.5 (**$p < 0.001$. Baseline** 15.8 ± 15.6 (**$p < 0.001$**)	**$p = 0.007$**	The algorithm is effective for correction of motion artefacts.
	DEBLUR (bilinear CNN model)	FLASH / $n = 5$	HFEN for **DEBLUR** 0.18±0.13, for **SToRM** 0.82 ± 0.05, for **Low-Rank** 1.23 ± 0.02	SSIM for **DEBLUR** 0.96 ± 0.04, for **SToRM** 0.59 ± 0.04, for **Low-Rank** 0.38 ± 0.02	Minimizes artefacts with limited data.
HM	Adversial Autoencoder network and unsupervised learning	bSSFP / $n = 4000$	Sharpness increase of motion –corrupted images by 7 % (Tenengrad focus measure) **$P < 0.05$**	**Baseline** SSIM (0.76), **Proposed** (0.93). **Baseline** image quality (2.5), **Proposed** (3.5), with breath-holds (4.1), (score out of 5.0)	Reduces respiratory motion artefacts, requires larger datasets.

Table 4
This table presents AI algorithms focused on image reconstruction.

AI model	AI algorithm name and architecture	MRI sequence/ subjects (n)	Reconstruction score	Image quality score	Clinical notes
CNN	**Unet** and **Resnet** networks	2D bSSFP / $n = 5$	1–5 ranking system (1=poor image quality, 5=excellent image quality), **Unet** mean rank=1.40, **Resnet** mean rank=2.44	**Unet** SNR (0.983–0.991), **Resnet** SNR (0.986- 0.994),**Unet** SSIM (0.964–0.980), **Resnet** SSIM (0.985–0.991) $\boldsymbol{P < 0.05}$	Can be used with limited training data, and accelerate image reconstruction, maintaining diagnostic quality
	MoCo-MoDL (RespME-net with motion informed MoDL network and MoCo, motion corrected, reconstruction)	CMRA / $n = 24$	1–4 scoring system (1=poor image quality, 4=excellent image quality), Mean score=3.56 ± 0.53, previous model (**PROST**) mean score=3.22 ± 0.44	PSNR (27.86 ± 3.00) SSIM (0.78 ± 0.06), previous model (**PROST**) PSNR (22.28 - 29.5) SSIM (0.65–0.81) $\boldsymbol{P < 0.05}$	Can reduce scan and reconstruction times, with diagnostic image quality
	DCCNN (deep cascade of convolutional neural networks, with data consistency and regularisation layers, U-net)	2D CINE / $n = 43$	MAE (0.04 ± 0.03) similar to previous method **XD-GRASP**, MAE (0.04 ± 0.02)	PSNR (30.9 ± 0.07), SSIM (0.90 ± 0.04); improved compared to previous used method **XD-GRASP**, PSNR (29.96 ± 0.07), SSIM (0.89 ± 0.04)	Improves scan time with diagnostic images quality
	CRNN (bidirectional recurrent unit, 3 convolution layers, with single image super-resolution refinement module)	CINE / $n = 300$	NMSE (0.0277 – 0.0408) improved to previous method (**Plain CRNN**), NMSE (0.0311 – 0.0464)	PSNR (28.644 – 30.295), SSIM (0.822 – 0.854); improved to previous method used (**Plain CRNN**), PSNR (28.030 – 29.842) SSIM (0.788 – 0.824)	Can improve the quality of reconstructed images
	k-t CLAIR (self-consistency guided, unrolled neural networks, multi-prior learning architecture)	CINE, T1/T2 W / $n = 120$	Avg. NMSE for CINE (0.0063), Avg. NMSE for T1/T2W (0.0035); improved to previous method (**E2EVarNet3D**) Avg. NMSE for CINE and T1/T2 (0.0074, 0.0048)	Avg. PSNR for CINE and T1/T2W (37.54, 38.43), Avg. SSIM for same seq. (0.9454, 0.9621); improved to **E2EVarNet3D**, Avg. PSNR (36.86, 37.39), Avg. SSIM (0.9394, 0.9561)	High quality image reconstruction for CINEs and T1/T2W
PG-DL	Zero shot **PG-DL** with spatio-temporal regularization	bSSP / $n = 11$	N/A	PSNR (33.71 ± 1.94), SSIM (89.76 ± 2.07 %); improved to the control method **LLR**-regularized reconstruction PSNR (28.14 ± 1.29), SSIM (81.44 ± 2.83 %) $\boldsymbol{P < 10-4}$	High quality and accelerated images
GAN	**SRGAN** (generative adversarial SR framework (single-image) combined together with non-rigid respiratory motion-compensation)	3D bSSFP (CMRA) / $n = 31$	NMAE ∼ 0.3, NMSE ∼ 0.01, improved to baseline **Bicubic interpolation** (NMAE ∼ 0.8, NMSE ∼ 0.09)	SSIM ∼ 0.925, improved to baseline **Bicubic interpolation** (SSIM ∼ 0.591) $\boldsymbol{P < 0.001}$	Fast 3D CINE with high resolution
HM	**DnSRGAN** (CNN for denoising (DnCNN), gradient penalty (GP), and SRGAN)	N/A $n = 64$	N/A	Avg-PSNR (30.1407), Avg-SSIM (0.9090); improved to previous models like **ESRGAN** Avg-PSNR (28.1024), Avg-SSIM (0.8339)	The model can perform super-resolution processing, and can denoise images
	MCMR (CG-SENSE and for image reconstruction and GRAFT (CNN module) for motion estimation)	2D bSSFP / $n = 886$	NMSE (0.058 - 0.193), improved to previous method (**GRAFT + CG-SENSE**), NMSE (0.097–0.302)	PSNR (31.964 - 41.7), SSIM (0.864 – 0.98); improved to previous method (**GRAFT + CG-SENSE**), PSNR (27.047 −37.305), SSIM (0.58 - 0.964)	Can obtain high quality reconstruction

(28.644–30.295), SSIM (0.822–0.854). k-t CLAIR obtained NMSE 0.0063 (CINE) and 0.0035 (T1/T2W), PSNR 37.54 and 38.43.

PG-DL: Zero-shot PG-DL for bSSFP achieved PSNR 33.71 ± 1.94 and SSIM 0.898 ± 0.021.

GAN: SRGAN for 3D bSSFP had NMAE ~0.3 and SSIM ~0.925.

HM: DnSRGAN achieved PSNR 30.14 and SSIM 0.909. Hybrid MCMR (CG-SENSE and GRAFT) for 2D bSSFP reported NMSE 0.058–0.193 and PSNR 41.7.

Of the 31 included studies, 17 were assessed as having a low risk of bias, while 14 were rated as moderate. No studies were classified as high risk. The most common limitations contributing to moderate risk were small or homogeneous sample sizes, lack of external validation, and reliance on retrospective or single-centre datasets.

Across the included studies, convolutional neural networks (CNNs) emerged as the predominant AI architecture. Key limitations frequently cited included small or heterogeneous datasets, which may constrain the generalisability and robustness of the findings. Notably, despite these constraints, the studies consistently reported comparable or superior image quality relative to conventional CMR acquisition and reconstruction techniques.

Image quality was assessed in the included studies using a combination of subjective radiologist scoring and quantitative metrics such as signal-to-noise ratio (SNR), structural similarity index (SSIM), peak signal-to-noise ratio (PSNR) and mean absolute error (MAE).

Discussion

In this section, a specific discussion for each of the categories analysed in the results will be presented.

Different deep learning architectures contribute in distinct ways to CMR image quality. CNNs excel at analysing and extracting information from images, making them particularly effective for artefact detection and reduction. U-Nets capture both global context and local detail, which is valuable for preserving cardiac anatomy. GANs are mainly employed to enhance sharpness and enable super-resolution. Each of these approaches offers unique strengths, and when combined, they can provide complementary benefits, leading to further improvements in image quality and diagnostic value [1,11,20].

Scan acceleration, including breath-hold shortening

One of the most challenging parts of a CMR test is the breath-hold requirement. Recently, researchers have trained and evaluated AI models to shorten the breath-hold, enable free breathing, and speed up CMR exams.

With these improvements, the CMR procedure can be performed in patients with difficulty breathing [7,9,10].

Both MoDL-SToRM and MoCo-MoDL showed strong performance in reducing scan time and breath-holds. MoDL-SToRM achieved fast reconstruction (≈30 s) with PSNR values of 37.83–42.98 and SSIM scores of 0.9021–0.9721, highlighting high image fidelity. In contrast, MoCo-MoDL demonstrated a dramatic scan time acceleration (≈240×; 2.1 ± 0.3 min) and high diagnostic confidence (median = 4/4) with excellent sharpness (median = 5/5), supported by an SSIM of 0.906. Together, these findings suggest MoDL-SToRM excels in reconstruction efficiency, while MoCo-MoDL prioritizes scan acceleration without compromising image quality [6,21].

The DIP-MRF algorithm reduced scan duration substantially (15 to 5 heartbeats; 250 ms to 150 ms) while maintaining diagnostic reliability. Mean T1 (1047 ± 46 ms) and T2 (45.7 ± 4.0 ms) values were consistent with reference standards, underscoring its ability to accelerate acquisition without compromising image quality [9]. The 2D convolutional CNN achieved reconstruction within approximately 9 s, providing satisfactory PSNR and SSIM values [20]. By comparison, 4D CINENet enabled CINE imaging in a similarly short time (≈10 s) while maintaining good image quality (as shown in Fig. 2) and providing a substantial improvement in image contrast (+67 %) relative to iterative reconstructions [2]. While both approaches demonstrate efficiency in reducing reconstruction time, 4D CINENet appears to offer additional benefits in image quality enhancement, though further validation is required for broader clinical application. The EasyScan model enables planning efficiency while increasing SNR and image sharpness and it also automates the shim volume [7]. CNN with 2D convolutional layers and 4D CINENet can achieve an optimal balance between speed and image quality, whereas EasyScan is suited for clinical efficiency [2,7].[22] Other AI algorithms, including DLR and variational networks, have also been tested and trained to accelerate CMR scans. DLR applied to standard 2D bSSFP reduces scan time from 327.6 ± 65.8 s to 41.0 ± 11.3 s, while preserving image contrast (standard bSSFP: 4.9 ± 0.3 vs DLR: 4.8 ± 0.4) and artefact scores (standard bSSFP: 4.5 ± 0.7 vs DLR: 4.8 ± 0.4), indicating maintained diagnostic quality [23]. Sonic DL CINE further shortens acquisition times to 21–76 s, compared with 150 ± 34 s for traditional CINE, without statistically significant differences in image quality ($p > 0.198$), demonstrating high diagnostic fidelity [24]. Overall, Sonic DL provides the fastest acquisition, while both approaches retain excellent image quality and minimal motion artefacts, making them practical for clinical use [23,24].

Variational networks have been used to reduce scan times with differing strengths. jMS-VNN achieves acquisition in 3 ± 1 min and reconstruction in 20 ± 2 s, with high PSNR (47.39 ± 2.5) and SSIM (0.72 ± 0.1), outperforming compressed sensing in image quality [10]. In contrast, GC-VN reconstructs CMRA in 35 s and MTC-BOOST in 19 s, offering 30 % and 47.2 % faster reconstruction, respectively, with a PSNR of 31.5 ± 2.7, representing a 29 % signal increase over prior methods [25]. Overall, jMS-VNN excels in image fidelity and structural preservation, while GC-VN prioritizes speed and signal enhancement [10,25]. CNNs offer a good balance between reconstruction quality and scan acceleration, DLR

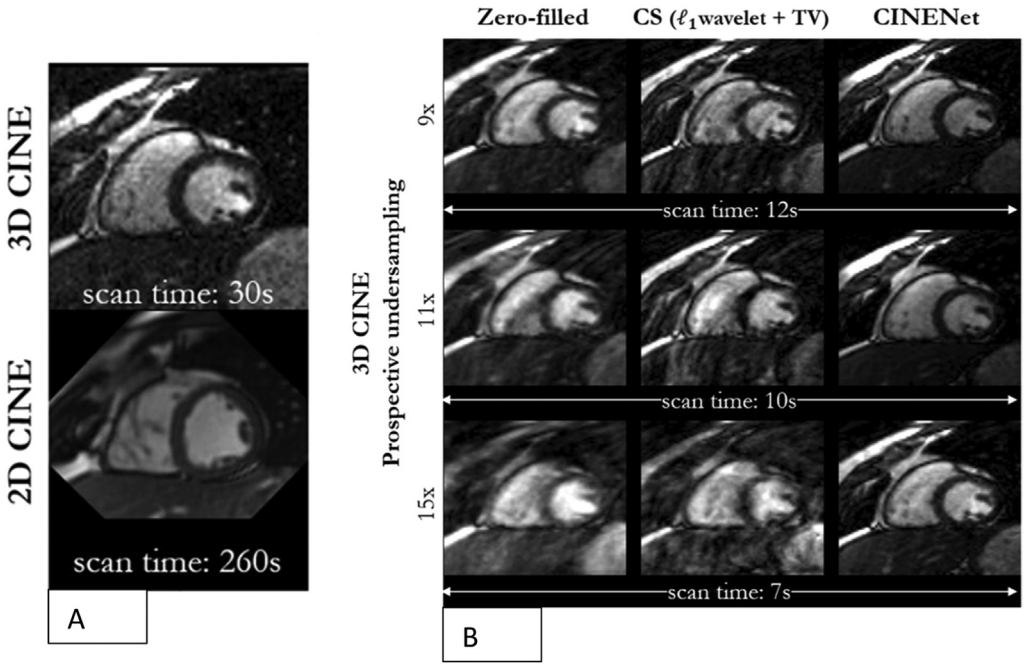

Fig. 2. The scan time of reference standard CINE CMR images 2D (260 s) and 3D (30 s with 2.5x acceleration factor using SENSE), (A). The scan time of the same image with an acceleration factor of 9x (12 s), 11x (10 s), 15x (7 s), and different reconstruction techniques, namely coil-weighted zero-filling (left column), Compressed Sensing (CS), central column, and proposed AI algorithm CINENet, right column (B) [2] ;.

methods achieve the fastest acquisitions while preserving diagnostic fidelity, and variational networks can be tuned to prioritize either image quality or reconstruction speed depending on clinical priorities [2,10,24].

Artefact detection

Several AI models have been designed to automate artefact detection with varying architectures and capabilities. Examples are IQ-DCNN, 3D ResNet-50, Hybrid Random Forest (Hyb-RF), and Deep Meta-Learning (DML). Each has unique strengths and limitations that make it suitable for a different clinical application [5,26,27].

IQ-DCNN shows strong reliability in identifying blurred images, matching expert performance in phase selection ($R^2 = 0.78$, kappa = 0.67), but it remains dependent on expert-verified reference images for clinical use [26]. By contrast, 3D ResNet-50 shows excellent performance in motion artefact detection in 2D b-SSFP CINE sequences (AUROC 0.87–0.90; overall 0.88–0.93), closely aligning with expert assessments and offering greater potential for clinical translation (as shown in Fig. 3) [18].

Hyb-RF detects inter-slice motion artefacts in 2D b-SSFP CINE with 78–85 % sensitivity and 90–95 % specificity, and shows high accuracy for contrast and coverage estimation (sensitivity 88–100 %, specificity 99–100 %) [27]. DML addresses respiratory and cardiac artefacts in 2D b-SSFP CINE and FIESTA, achieving accuracy of 56.51–99.28 %, precision of 55.43–99.46 %, and F-measure of 55.06–99.36 %. While it outperforms the compared models in artefact detection, it requires larger datasets for broader applicability [5]. CNN-based models (IQ-DCNN, 3D ResNet-50) show strong alignment with expert assessments, making them well-suited for artefact detection tasks, though IQ-DCNN remains dependent on expert-verified references. Hyb-RF demonstrates high sensitivity and specificity, particularly for inter-slice artefacts, but its scope is narrower. DML offers broader applicability across respiratory and cardiac artefacts and outperforms other models in precision, though it requires larger datasets for reliable clinical use [5,18,26,27].

Artefact reduction

Many AI models, such as CNNs and hybrid CNNs/Adversary autoencoder networks, have been evaluated to remove CMR artefacts, thus improving image quality and diagnosis [8,19,28].

CNN-based models demonstrate strong performance across different CMR artefact correction tasks. With CINE sequences, 3D CNN and LRCN achieve high motion artefact detection and correction (recall scores 467 ± 82 and 533 ± 65; precision scores 713 ± 69 and 724 ± 57; ROC 0.89) [28]. In PCMR sequences, U-Net improves edge definition and suppresses deep artefacts with MAE 0.0417 and SSIM 0.85, even across variable resolutions and FOVs without extra training [29]. A combined CNN/CRNN/U-Net approach further enhances segmentation accuracy (overlaps: LV 0.964, myocardium 0.775, RV 0.933) while increasing SSIM from 0.623 to 0.793 [11]. RT U-Net on bSSFP reduces reconstruction time with strong artefact scores (motion 4.3 ± 0.46;

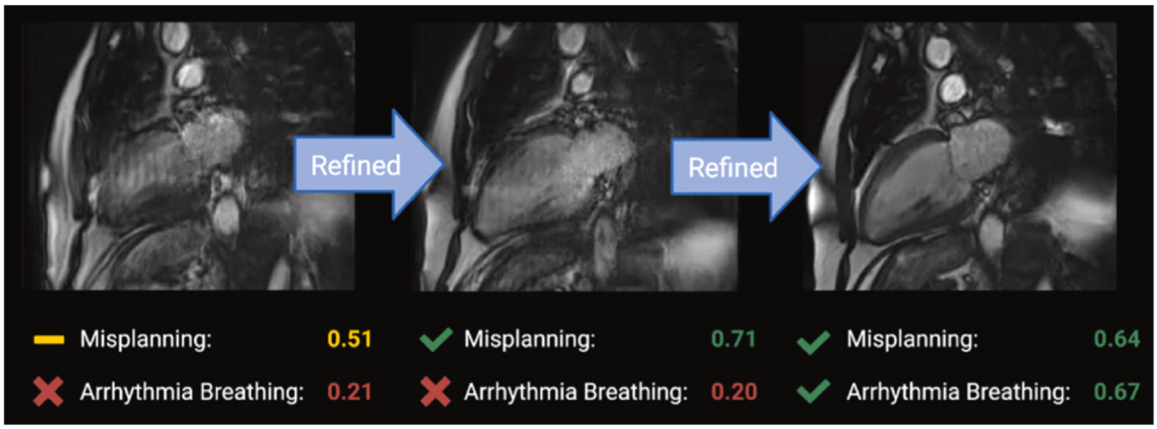

Fig. 3. Example of an AI-based automated image quality control assessment. The three images show 2-chamber CMR cine views with varying AI-generated quality scores. The AI algorithm iteratively assesses image quality by analysing factors such as MR sequence planning and the presence of motion artefacts, providing radiographers with actionable feedback to improve image quality [18].

general 4.6 ± 0.49) decreasing scan time without sacrificing image quality (as shown in Fig.4), meanwhile residual U-Net reconstructions achieve MAE <0.05 and SSIM 0.7–1 [19,29]. Other models extend utility: MOCOnet lowers motion scores from 37.1 ± 21 to 13.3 ± 10.5 ($p < 0.001$) on ShMOLLI T1 maps, and DEBLUR achieves HFEN 0.18 ± 0.13 and SSIM 0.96 ± 0.04 for FLASH sequences on small datasets [30,31].

These models reflect the versatility and efficiency of CNNs for dealing with multiple types of artefacts and enhancing CMR image quality.

For bSSFP sequences, HM uses an adversarial autoencoder with unsupervised learning, improving sharpness by 7 % (Tenengrad) and SSIM from 0.76 to 0.93. It shows potential to reduce breathing-related artefacts but requires larger datasets for clinical adoption [32].

3D CNN and LRCN stand out for reliable motion artefact detection and correction in CINE imaging, while U-Net variants excel in artefact suppression and generalizability [28,29]. Combined CNN–CRNN–U-Net models strengthen segmentation accuracy, making them suitable for structural analysis. RT U-Net and residual U-Net are efficient for rapid reconstruction with strong artefact reduction, whereas MOCOnet focuses on motion correction in T1 mapping, and DEBLUR is particularly effective for artefact correction in smaller datasets [11,29,30,31]. HM shows promise for addressing breathing-related artefacts but needs larger datasets for clinical translation [32].

Taken together, CNN-based approaches offer flexibility across artefact types, adaptability to different imaging sequences, and the capacity to balance reconstruction speed with high image quality. This versatility makes CNNs particularly valuable for artefact reduction in CMR, where both accuracy and efficiency are critical [11,28,31].

Image reconstruction

In CMR, various AI frameworks, including CNNs, recurrent layers, generative adversarial networks (GANs), and hybrid systems, can optimize image reconstruction. Some of these frameworks use algorithms that can detect motion artefacts, sharpen edges, and minimise noise to improve the image reconstruction and signal to noise ratio (SNR) [4,33,34].

The Unet and ResNet networks used for 2D bSSFP have a mean SNR of 0.983–0.994 and SSIM of 0.964–0.991. Unet ranks lower on a 1–5 scale in reconstruction quality (1.40) than ResNet (2.44), but both excel in maintaining diagnostic quality with limited data [33]. MoCo-MoDL for CMRA sequences similarly presents improved PSNR (27.86 ± 3.00) and SSIM (0.78 ± 0.06), surpassing the previous PROST model with a mean quality score of 3.56 ± 0.53 (on a 1–4 scale). This model significantly shortens the scan and reconstruction times [25].

For 2D CINE sequences, the DCCNN can provide PSNR of 30.9 ± 0.07 and SSIM of 0.90 ± 0.04, surpassing XD-GRASP (PSNR: 29.96, SSIM: 0.89) while maintaining a similar MAE (0.04 ± 0.03), [1]. In contrast, CRNN has NMSE values of 0.0277–0.0408, higher than standard CRNN (0.0311–0.0464), PSNR of 30.295 and SSIM of 0.854, further enhancing image reconstruction quality [4].

The k-t CLAIR model performs exceptionally for CINE and T1/T2-weighted sequences. It achieves NMSEs of 0.0063 (CINE) and 0.0035 (T1/T2W) and PSNR of 37.54 (CINE) and 38.43 (T1/T2W), outperforming the E2EVarNet3D baseline [34]. When reconstructing images obtained from bSSFP sequences, zero-shot PG-DL can achieve PSNR scores of 33.71 ± 1.94 and SSIM values of 89.76 ± 2.07 %, outperforming the compared LLR-regularized method [35].

Generative adversarial networks, such as SRGAN, further improve 3D bSSFP (CMRA) reconstructions (as shown in Fig.5), with NMAE scores of ∼0.3 and SSIM values of ∼0.925, significantly superior to Bicubic interpolation (SSIM: ∼0.591) [20]. Similarly, DnSRGAN, an algorithm for super-resolution and denoising, produces an average PSNR of 30.1407 and SSIM of 0.9090, which is superior to the compared method ESRGAN [36]. In this method, a DnCNN is used to denoise the images, and then the SRGAN performs the super-resolution

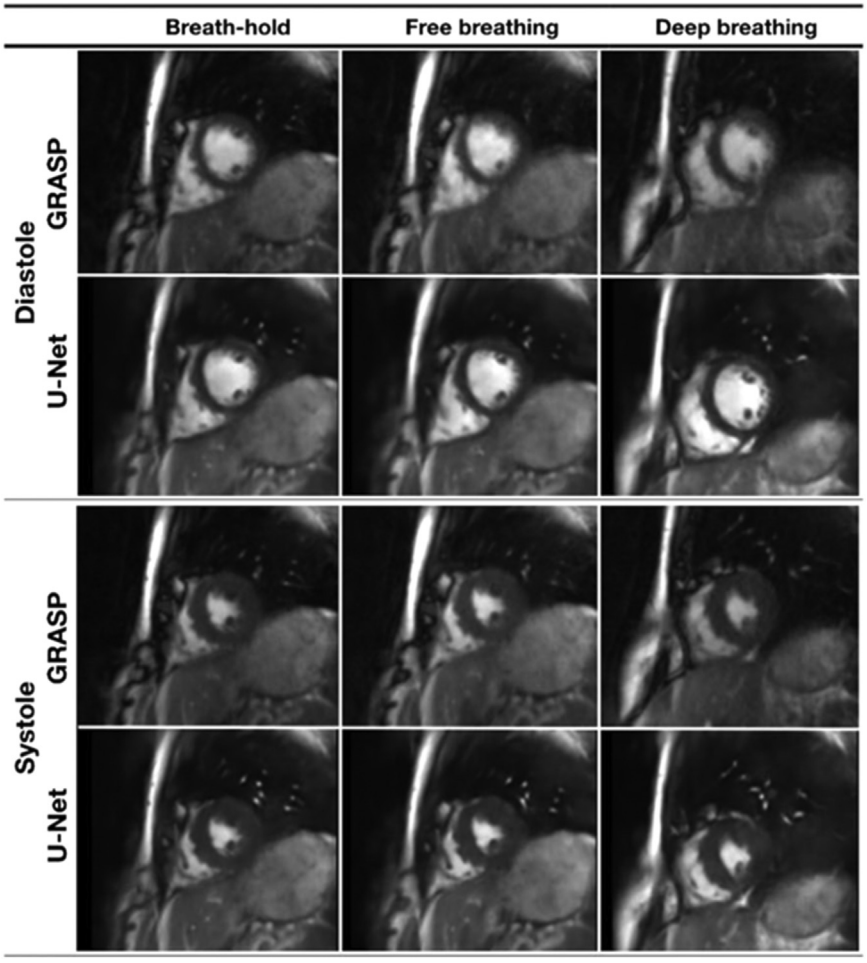

Fig. 4. Short-axis CMR image with motion artefact and artefact correction performed by GRASP compared with artefact correction technique performed by AI proposed U-Net algorithm [19].

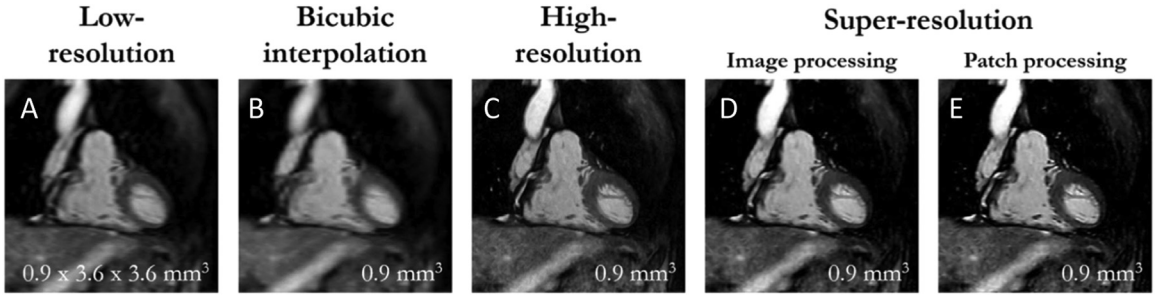

Fig. 5. Examples of 3D isotropic coronary MR angiography images obtained using different techniques and resolutions. The first image (A) has been obtained with low resolution, the second (B) with bicubic interpolation, the third (C) with high resolution, and the last two (D, E) with AI-based super-resolution reconstruction techniques [20].

reconstruction. This approach can be very effective because combining the CNN with the GAN architectures makes it possible to remove the noise and artefacts that often cause the CMR images to not be reconstructed properly during the super-resolution process.

The hybrid MCMR model (CG-SENSE and GRAFT), applied to 2D bSSFP, presents decreased NMSE (0.058–0.193) and raised PSNR (41.7) still providing good quality image reconstruction [37].

The strengths of these AI models vary. ResNet and Unet are best for small training data, while MoCo-MoDL and DCCNN improve speed and diagnostic accuracy. CRNN and k-t CLAIR provide the best image quality, while GAN models such as SR-GAN and DnSRGAN provide better resolution and noise control. Hybrid approaches such as MCMR can combine motion artefact correction with reconstruction quality [20,25,35].

The overall risk of bias was generally low, though nearly half of the studies had moderate risk due to limited datasets, lack

of external validation, or single-centre designs. While AI shows strong potential to improve CMR image quality, further multicentre, prospective validation is needed before clinical adoption.

Methodological challenges due to the sample characteristics

Some sample characteristics were present, which prevented direct comparisons in the eligible papers:

1) One of them is that some of the studies in the scoping review use data sets that are either too small or not homogeneous enough to generalise their findings [6].
2) Another challenge of the included literature is that AI models were typically tested on a single scanner type or imaging sequence, with few studies investigating transfer learning or domain adaptation to improve generalizability. Future research specifically designed to assess model performance across multiple scanners and imaging protocols is needed to address this gap [20].
3) Another issue is that the findings reported from different studies are not uniform. Non standardized evaluations, research methods, and formats make comparing research and drawing robust conclusions difficult [30,35]. It should be noted that the definition and assessment of image quality varied across studies, which may contribute to heterogeneity in the reported outcomes.

Future work

Given the speed at which AI develops, it was not feasible to assess generative AI use in CMR, but this might be something very relevant in the immediate future.

Limitations

This review has some limitations.

The search was performed PubMed, Google Scholar, arXiv, and the Cochrane Library to comprehensively capture relevant biomedical and technical studies. While EMBASE and IEEE Xplore may contain additional relevant records, they were not searched due to database overlap and access restrictions; this represents a limitation of our review.

To ensure feasibility, the review was restricted to English-language publications. We acknowledge that this restriction may introduce language bias and potentially exclude relevant evidence published in other languages.

Furthermore disagreements between reviewers during data extraction and quality assessment were resolved through discussion and consensus, with a third author consulted when necessary. Inter-rater agreement was not formally quantified using a kappa coefficient, which may represent a methodological limitation.

Conclusion

AI has the potential to streamline different aspects of CMR, impacting scan times, image quality and patient comfort [6]. AI acceleration techniques can accelerate scans, requiring few or no breath holds. They are especially useful for patients who struggle to hold their breath for a prolonged period of time [23]. These improvements save time, prevent motions artefacts and may, therefore, enhance image quality [7,10]. AI can identify and correct image artefacts [26]. CNNs, GANs, and hybrid algorithms can detect and remove artefacts during image acquisition and enhance image quality, making scans more accurate and interpretable [18,29].

AI can also assist in image reconstruction by minimising reconstruction time, filter noise from images, and optimise the resolution, thus maximizing the quality of the entire process [1,4,20]. Most AI applications reviewed remain at the technical proof-of-concept stage. Although the results are promising, further studies are required to validate these approaches across larger and more diverse datasets and to establish their readiness for integration into routine clinical workflows [7,8,21].

Acknowledgements

The main author gratefully acknowledge the invaluable support provided by Alliance Medical throughout the course of this MSc project. Their guidance, resources, and facilitation were instrumental in the successful completion of the research, enabling the development and publication of this scoping review.

Supplementary materials

Supplementary material associated with this article can be found, in the online version, at doi:10.1016/j.jmir.2025.102135.

References

[1] Machado I, Puyol-Anton E, Hammernik K, Cruz G, Ugurlu D, Olakorede I, Oksuz I, Ruijsink B, Castelo-Branco M, Young A, Prieto C, Schnabel J, King A. A deep learning-based integrated framework for quality-aware undersampled cine cardiac MRI reconstruction and analysis. *IEEE Trans Biomed Eng*. 2024;71(3):855–865. doi:10.1109/TBME.2023.3321431.
[2] Küstner T, Fuin N, Hammernik K, Bustin A, Qi H, Hajhosseiny R, Masci PG, Neji R, Rueckert D, Botnar RM, Prieto C. CINENet: deep learning-based 3D cardiac CINE MRI reconstruction with multi-coil complex-valued 4D spatio-temporal convolutions. *Sci Rep*. 2020;10:13710. doi:10.1038/s41598-020-70610-0.
[3] Qi H, Fuin N, Kuestner T, Botnar R, Prieto C, et al. Accelerated 4D respiratory motion-resolved cardiac MRI with a model-based variational network. In: Martel AL, Abolmaesumi P, Stoyanov D, Mateus D, Zuluaga MA, Zhou SK, et al., eds. *Medical Image Computing and Computer-Assisted Intervention – MICCAI 2020*. Cham: Springer; 2020:427–435. doi:10.1007/978-3-030-59725-2_41.
4 Xue Y, Du Y, Carloni G, Pachetti E, Jordan C, Tsaftaris SA. Cine cardiac MRI reconstruction using a convolutional recurrent network with refinement. *arXiv*. 2023;2309:13385. doi:10.48550/arXiv.2309.13385.
[5] Nabavi S, Simchi H, Ebrahimi Moghaddam M, Abin AA, Frangi AF. A generalised deep meta-learning model for automated quality control

of cardiovascular magnetic resonance images. *Comput Methods Programs Biomed*. 2023;242:107770. doi:10.1016/j.cmpb.2023.107770.
[6] Phair A, Fotaki A, Felsner L, Fletcher TJ, Qi H, Botnar RM, Prieto C. A motion-corrected deep-learning reconstruction framework for accelerating whole-heart magnetic resonance imaging in patients with congenital heart disease. *J Cardiovasc Magn Reson*. 2024;26(1):101039. doi:10.1016/j.jocmr.2024.101039.
[7] Edalati M, Zheng Y, Watkins MP, Chen J, Liu L, Zhang S, Song Y, Soleymani S, Lenihan DJ, Lanza GM. Implementation and prospective clinical validation of AI-based planning and shimming techniques in cardiac MRI. *Med Phys*. 2022;49(1):129–143. doi:10.1002/mp.15327.
[8] Jaubert O, Steeden J, Montalt-Tordera J, Arridge S, Kowalik GT. Muthurangu V. Deep artifact suppression for spiral real-time phase contrast cardiac magnetic resonance imaging in congenital heart disease. *Magn Reson Imaging*. 2021;83:125–132. doi:10.1016/j.mri.2021.08.005.
[9] Hamilton JI. A self-supervised deep learning reconstruction for shortening the breathhold and acquisition window in cardiac magnetic resonance fingerprinting. *Front Cardiovasc Med*. 2022;9:928546. doi:10.3389/fcvm.2022.928546.
[10] Fotaki A, Fuin N, Nordio G, Velasco Jimeno C, Qi H, Emmanuel Y, Pushparajah K, Botnar RM, Prieto C. Accelerating 3D MTC-BOOST in patients with congenital heart disease using a joint multi-scale variational neural network reconstruction. *Magn Reson Imaging*. 2022;92:120–132. doi:10.1016/j.mri.2022.06.012.
[11] Oksuz I, Clough JR, Ruijsink B, Puyol Anton E, Bustin A, Cruz G, Prieto C, King AP, Schnabel JA. Deep learning-based detection and correction of cardiac MR motion artefacts during reconstruction for high-quality segmentation. *IEEE Trans Med Imaging*. 2020;39(12):4001–4010. doi:10.1109/TMI.2020.3008930.
[12] JBI. *Checklist For Systematic Reviews and Research Syntheses*. JBI; 2020. PublishedAug. Available from: https://sites/default/files/2020-08/Checklist_for_Systematic_Reviews_and_Research_Syntheses.pdfAccessed 2024 Jun 12.
[13] Moher D, Liberati A, Tetzlaff J, Altman DG. Preferred reporting items for systematic reviews and meta-analyses: the PRISMA statement. *PLoS Med*. 2009;6(7):e1000097 Jul 21Epub 2009 Jul 21. doi:10.1371/journal.pmed.1000097.
[14] Teesside University. PICO process. Available at: https://tees.ac.uk/lis/learninghub/cinahl/pico.pdf [Accessed: 12 Jan 2025].
[15] PROSPERO. International prospective register of systematic reviews. Available at: https://www.crd.york.ac.uk/prospero/[Accessed: 12 Jan 2025].
[16] Flemming K, Booth A, Garside R, Tunçalp Ö, Noyes J. Qualitative evidence synthesis for complex interventions and guideline development: clarification of the purpose, designs and relevant methods. *BMJ Glob Health*. 2019;4:e000882. doi:10.1136/bmjgh-2018-000882.
[17] Critical Appraisal Skills Programme (CASP). CASP tools and checklists. Available at: https://casp-uk.net/casp-tools-checklists/[Accessed: 12 Jan 2025].
[18] Cheung HC, Vimalesvaran K, Zaman S, Michaelides M, Shun-Shin MJ, Francis DP, Cole GD, Howard JP. Automating quality control in cardiac magnetic resonance: artificial intelligence for discriminative assessment of planning and motion artifacts and real-time reacquisition guidance. *J Cardiovasc Magn Reson*. 2024;26(2):101067. doi:10.1016/j.jocmr.2024.101067.
[19] Hauptmann A, Arridge S, Lucka F, Muthurangu V, Steeden JA. Real-time cardiovascular MR with spatio-temporal artifact suppression using deep learning-proof of concept in congenital heart disease. *Magn Reson Med*. 2019;81(2):1143–1156. doi:10.1002/mrm.27480.
[20] Küstner T, Munoz C, Psenicny A, Bustin A, Fuin N, Qi H, Neji R, Kunze K, Hajhosseiny R, Prieto C, Botnar R. Deep-learning based super-resolution for 3D isotropic coronary MR angiography in less than a minute. *Magn Reson Med*. 2021;86(5):2837–2852. doi:10.1002/mrm.28911.
[21] Biswas S, Aggarwal HK, Jacob M. Dynamic MRI using model-based deep learning and SToRM priors: moDL-SToRM. *Magn Reson Med*. 2019;82(1):485–494. doi:10.1002/mrm.27706.
[22] Kofler A, Dewey M, Schaeffter T, Wald C, Kolbitsch C. Spatio-temporal deep learning-based undersampling artefact reduction for 2D radial cine MRI with limited training data. *IEEE Trans Med Imaging*. 2020;39(3):703–717. doi:10.1109/TMI.2019.2930318.
[23] Orii M, Sone M, Osaki T, Kikuchi K, Sugawara T, Zhu X, Janich MA, Nozaki A, Yoshioka K. Reliability of respiratory-gated real-time two-dimensional cine incorporating deep learning reconstruction for the assessment of ventricular function in an adult population. *Int J Cardiovasc Imaging*. 2023;39(5):1001–1011. doi:10.1007/s10554-023-02793-2.
[24] Chanda A., Milshteyn E., Tysarowski M., Nadig V. Use of DL reconstruction for highly undersampled CINE images in patients with cardiomyopathy. Abstract Volume. 2024;26(Suppl 1):815S1-926.
[25] Qi H, Hajhosseiny R, Cruz G, Kuestner T, Kunze K, Neji R, Botnar R, Prieto C. End-to-end deep learning nonrigid motion-corrected reconstruction for highly accelerated free-breathing coronary MRA. *Magn Reson Med*. 2021;86(4):1983–1996. doi:10.1002/mrm.28851.
[26] Piccini D, Demesmaeker R, Heerfordt J, Yerly J, Di Sopra L, Masci PG, Schwitter J, Van De Ville D, Richiardi J, Kober T, Stuber M. Deep learning to automate reference-free image quality assessment of whole-heart MR images. *Radiol Artif Intell*. 2020;2(3):e190123. doi:10.1148/ryai.2020190123.
[27] Tarroni G, Oktay O, Bai W, Schuh A, Suzuki H, Passerat-Palmbach J, de Marvao A, O'Regan DP, Cook S, Glocker B, Matthews PM, Rueckert D. Learning-based quality control for cardiac MR images. *IEEE Trans Med Imaging*. 2019;38(5):1127–1138. doi:10.1109/TMI.2018.2878509.
[28] Oksuz I, Ruijsink B, Puyol-Antón E, Clough JR, Cruz G, Bustin A, Prieto C, Botnar R, Rueckert D, Schnabel JA, King AP. Automatic CNN-based detection of cardiac MR motion artefacts using k-space data augmentation and curriculum learning. *Med Image Anal*. 2019. doi:10.1016/j.media.2019.04.009.
[29] Jaubert O, Montalt-Tordera J, Knight D, Coghlan GJ, Arridge S, Steeden JA, Muthurangu V. Real-time deep artifact suppression using recurrent U-nets for low-latency cardiac MRI. *Magn Reson Med*. 2021;86(4):1904–1916. doi:10.1002/mrm.28834.
[30] Gonzales RA, Zhang Q, Papież BW, Werys K, Lukaschuk E, Popescu IA, Burrage MK, Shanmuganathan M, Ferreira VM, Piechnik SK. MOCOnet: robust motion correction of cardiovascular magnetic resonance T1 mapping using convolutional neural networks. *Front Cardiovasc Med*. 2021;8:768245. doi:10.3389/fcvm.2021.768245.
[31] Ahmed AH, Zou Q, Nagpal P, Jacob M. Dynamic imaging using deep bilinear unsupervised representation (DEBLUR). *IEEE Trans Med Imaging*. 2022;41(10):2693–2703. doi:10.1109/TMI.2022.3168559.
[32] Ghodrati V, Bydder M, Ali F, Gao C, Prosper A, Nguyen K-L, Hu P. Retrospective respiratory motion correction in cardiac cine MRI reconstruction using adversarial autoencoder and unsupervised learning. *NMR Biomed*. 2021;34(2):e4433. doi:10.1002/nbm.4433.
[33] Ghodrati V, Shao J, Bydder M, Zhou Z, Yin W, Nguyen K-L, Yang Y, Hu P. MR image reconstruction using deep learning: evaluation of network structure and loss functions. *Quant Imaging Med Surg*. 2019;9(9):1516–1527. doi:10.21037/qims.2019.08.10.
[34] Zhang L., Chen W. k-t CLAIR: self-consistency guided multi-prior learning for dynamic parallel MR image reconstruction. arXiv. 2023; 2310.11050. doi:10.48550/arXiv.2310.11050.
[35] Demirel ÖB, Zhang C, Yaman B, Gulle M, Shenoy C, Leiner T, Kellman P, Akçakaya M. High-fidelity database-free deep learning reconstruction for real-time cine cardiac MRI. *bioRxiv*. 2023. doi:10.1101/2023.02.13.528388.
[36] Zhao M, Wei Y, Wong KKL. A generative adversarial network technique for high-quality super-resolution reconstruction of cardiac magnetic resonance images. *Magn Reson Imaging*. 2022;85:153–160. doi:10.1016/j.mri.2021.10.033.
[37] Pan J, Hamdi M, Huang W, Hammernik K, Kuestner T, Rueckert D. Unrolled and rapid motion-compensated reconstruction for cardiac CINE MRI. *Med Image Anal*. 2024;91:103017. doi:10.1016/j.media.2023.103017.